Influence of nanoparticle surfaces on the electrical breakdown strength of nanoparticle-filled low-density polyethylene

Dongling Ma, Richard W. Siegel, Jung-Il Hong, and Linda S. Schadler
Materials Science and Engineering Department and Rensselaer Nanotechnology Center, Rensselaer Polytechnic Institute, Troy, New York 12180

Eva Mårtensson and Carina Önneby
ABB AB, Department H, Västerås, S-721 78, Sweden

(Received 29 September 2003; accepted 25 November 2003)

The electrical breakdown strength of TiO_2 nanoparticle-filled low-density polyethylene (LDPE) nanocomposites was investigated. It was found that the surface water on the nanoparticles played a very important role in determining the breakdown strength. The breakdown strength at 63.2% cumulative failure probability (E_0) for the composites filled with dried nanoscale TiO_2 was similar to that of neat LDPE and 50% higher than that for the samples filled with as-received nanoscale TiO_2. This increase was due to a better dispersion, a better interface, and a morphology change of the matrix. It was also found that surface modification of nanoscale TiO_2 had a significant influence on the breakdown strength. *N*-(2-aminoethyl) 3-aminopropyl-trimethoxysilane (AEAPS)-coated TiO_2-filled samples showed about 40% higher E_0 than that of uncoated, as-received TiO_2-filled samples. This was mainly due to enhanced electron scattering because of the presence of polar groups in AEAPS.

I. INTRODUCTION

Polymers play an important role in electrical insulating technology because of their high electrical strength, ease of fabrication, low cost, and simple maintenance.[1–3] Conventionally, additives have been mixed into polymer matrices to improve their resistance to degradation,[4] to modify mechanical and thermomechanical properties,[5] and to improve electrical properties such as high-field stability.[6] One limitation of conventional additives is the negative effect they can have on breakdown strength. In the ideal case, an additive will both modify the property of interest and increase the breakdown strength or at least not degrade it.

An example of an additive that can improve the breakdown strength is azocompounds.[7] The azocompounds used consist of a benzene or naphthalene ring to which one or more radicals are connected. A radical is either an electron acceptor or electron donor. The increase of the breakdown strength is due to the trapping and the excitation effect of this additive. On the other hand, plasticizers tend to cause a marked reduction of the breakdown strength.[8] This is because the plasticizer increases the free volume of the polymer, thus leading to an increase in the electron mean free path causing early breakdown. Both of these kinds of additives exist in polymer matrices in their molecular state. Once the additive appears as a separate phase (e.g., particles) in the polymer matrix, local field distortion becomes an important factor, and in most cases such additive particles cause a decrease in the breakdown strength of insulating materials.[9–11] A second phase can also influence the breakdown strength via a tortuosity mechanism (i.e., an increase in the path length of the breakdown)[12] or by changing the space charge distribution.[13]

Under alternating current (ac) conditions, local field distortion and enhancement is caused by the difference in permittivity between the additive particles and the polymer matrix whereas under direct current (dc) conditions, the local field distortion is caused by the difference in conductivity between the additive particles and the polymer. In these cases, the additive particles act as local field enhancing defect centers. When the same kinds of particles, which have the same permittivity or conductivity and shape, are used, the local field distortion is only determined by the size of the particles. The larger the particles are, the greater the possibility of a large field enhancement. Therefore, nanoparticles are expected to result in less of a loss in breakdown strength than traditional microparticles. In this paper, we explore the effect of particle size and surface state on breakdown strength of polyethylene under dc conditions.

II. EXPERIMENTAL

The matrix used in this study was low-density polyethylene (LDPE) DOW Chemical Company (Midland,

MI) 681I. The basic characteristics of LDPE 681I were density 0.922 g/cc and melt index 1.2 g/10 min. Both microscale (1–2 μm) from Alfa Aesar (Ward Hill, MA) and nanoscale (23-nm average diameter) TiO_2 from Nanophase Technologies Corporation (Burr Ridge, IL) were used as additives. Five wt% TiO_2 particles were mixed into LDPE at 130 °C with net mixing time of 10 min in a Haake System 90 Buchler (Saddle Brook, NJ) mixer. Films with a thickness of 10–40 μm were obtained using compression molding at 160 °C under a pressure of about 14 MPa. The temperature of the film was decreased to 50–60 °C slowly in the mold under pressure before it was removed from the mold and air-cooled to room temperature. Each sample was then kept in a desiccator for at least 1 day before the breakdown strength was measured in case residual internal stresses influence the experimental results. According to our dynamic mechanical analysis, the glass transition temperature of neat LDPE was about –120 °C, so room temperature was high enough for molecular relaxation in the polymer matrix to occur. Unfilled LDPE went through exactly the same process to make the results comparable between neat and filled polymer samples. TiO_2 particles with three different surface conditions were used: as received, vacuum dried at 195 °C for 24 h, and surface modified. Both the dried and surface-modified particles were ground before being mixed into the matrix to break up large agglomerates.

The surface modification was carried out by toluene reflux. *N*-(2-aminoethyl) 3-aminopropyl-trimethoxysilane (AEAPS) from Gelest. Inc. (Tulleytown, PA) was used as a coupling agent. Toluene was first dried by CaH_2 powder in N_2 atmosphere and purified by distillation. Five grams of dried nanoscale TiO_2 were dispersed by sonication (Sonics Vibracell, Newtown, CT, 750 W) at 70% power for 5 min in dried toluene. Coupling agent was slowly added to the nanoscale TiO_2/toluene mixture. Then, the mixture was put into an oil bath at 135 °C and magnetically stirred for 48 h under dry air atmosphere. The resulting slurry was centrifuged at 6000 rpm for 10 min and then washed twice with fresh toluene. Finally, the modified particles were dried in a vacuum oven at about 30 °C for 24 h.

A sphere-plane setup[14] was used for the breakdown measurements. The diameter of the sphere was ¼ inch (0.64 cm). The spherical electrode was connected to a high potential whereas the plane electrode was connected to ground potential. The test was performed at room temperature using a stepwise voltage. Each voltage step was 100 V and was maintained for approximately 1 s before the high voltage electrode was grounded and the next higher voltage was applied. The process proceeded until breakdown occurred showing a sharp current increase. Breakdown strength was calculated as the electrical voltage divided by the sample thickness.

A Weibull distribution was used to analyze the breakdown data. This distribution has been found to be the most appropriate for electrical strength analyses, and it is described in detail elsewhere.[10,15] The cumulative probability P of the electrical failure takes the form of

$$P = 1 - \exp\left[-\left(\frac{E}{E_0}\right)^{\beta}\right] \quad , \tag{1}$$

where β is a shape parameter and E_0 is a scale parameter that represents the breakdown strength at the cumulative failure probability of 63.2%. P is defined as[15]

$$P_i = \frac{i - 0.5}{n + 0.25} \quad , \tag{2}$$

where i is the ith result when the values of E are sorted in ascending order, and n is the number of measurements. Both β and E_0 were obtained from linear regression of the linearized Eq. (1)

$$\log[-\ln(1 - P)] = \beta \log E - \beta \log E_0 \quad . \tag{3}$$

We use E_0 to show the significance in the differences between several sets of breakdown data.

Thermogravimetric analysis (TGA) was performed on a Mettler (Toledo, Switzerland) TGA/SDTA in air for coated particles and in nitrogen for water content determination of pure particles at the rate of 20 °C/min. Field emission scanning electron microscopy (FE-SEM) was used with a JEOL (Tokyo, Japan) JSM-6330F to observe the particle dispersion status. The surface of thin film samples was checked under FE-SEM directly after being etched by O_2 plasma for 1 h for surface dispersion whereas the internal dispersion was examined by looking at the cross section of thin-film samples broken in liquid nitrogen. Differential scanning calorimetry (DSC) experiments were carried out on a Mettler DSC 822e with ramp rate at 10 °C/min. Thin-film samples ranging in weight from 3 to 6 mg were used. Data from the first melting-run involving thermal history information was used in this research. Lamellae thickness distribution was approximated by using the following equation[16]

$$g(l) = KP(T)(T_m^0 - T)^2 \quad , \tag{4}$$

where l is lamellar thickness, $g(l)$ is a lamellae thickness distribution function, $P(T)$ is the heat flow obtained from DSC, T_m^0 is the melting temperature of a perfect crystal with a value of 418.7 K for polyethylene, and K is a function of heating rate, surface energy, molecular weight, crystal density, and mass degree of crystallinity, and it is independent of temperature. Thus, K can be obtained by normalizing $g(l)$. The relationship between melting temperatures and lamellae thicknesses is simplified to the Thompson–Gibbs equation[16]

$$T_m = T_m^0\left(1 - \frac{2\sigma}{\Delta H_v l}\right) \quad , \tag{5}$$

where the surface energy σ is equal to 90 mJ/m^2 and the heat of fusion per unit volume ΔH_v is equal to 286,232 kJ/m^3 for polyethylene. See Ref. 16 for detailed information.

X-ray diffraction (XRD) was done on a Scintag (Cupertino, CA) XDS 2000. Peak areas A of amorphous and crystalline (110) and (200) were obtained from curve-fitting. The equation used for crystallinity α_c is[17]

$$\alpha_c = \frac{A_{110} + 1.46 \times A_{200}}{A_{110} + 1.46 \times A_{200} + 0.75 \times A_{\text{amorphous}}} \quad . \quad (6)$$

Tapping mode atomic force microscopy (AFM) was used to visualize matrix morphology. Both height and phase images were simultaneously obtained on a Digital Instruments (Santa Barbara, CA) Nanoscope III microscope using silicon cantilevers having a spring constant of 40 N/m. Experiments were conducted at room temperature. Samples were prepared by remelting the thin-film samples made by following the above-described procedures and then crystallized with a free surface from 160 to 50 °C in the mold on the press. The cooling process was the same as that used to prepare the thin-film samples for breakdown tests except that no pressure was applied to the AFM samples.

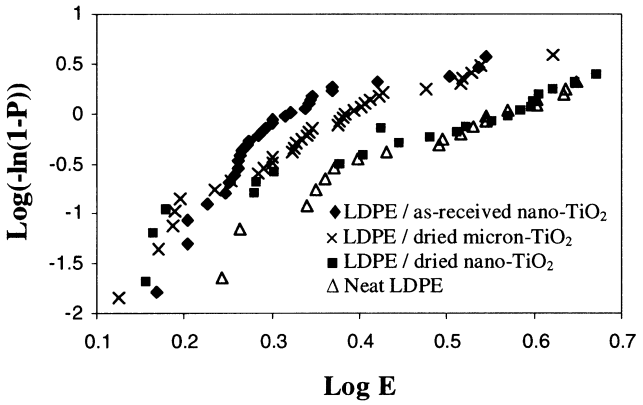

FIG. 1. Linear regression of the Weibull distribution of the electrical breakdown strength.

III. RESULTS AND DISCUSSION

Electrical breakdown strength is defined as the electric-field intensity that causes an "insulator-to-conductor" transition in a material and is accompanied by a sharp increase in current. Figure 1 shows the Weibull plots of the breakdown strength of neat LDPE samples and of the composite samples containing as-received nanoscale TiO_2, dried nanoscale TiO_2, or dried microscale TiO_2 particles. The difference in E_0 obtained from the linear regression of the Weibull plot for these four kinds of samples is clearly shown in Table I.

Neat LDPE had an E_0 of 3.78 MV/cm. Although it was lower than most reported data for phosphatidyl ethanolimine, depending on the brand of PE, lower values have been shown.[18] In addition, as demonstrated in Ref. 14, the test geometry has a significant influence on breakdown strength, and the sphere-plane geometry reveals the lowest breakdown strength. With the incorporation of 5 wt% as-received nanoscale TiO_2, a 40% decrease in the breakdown strength was observed as compared to neat LDPE. A 95% confidence interval (not shown here) indicated that this difference was significant. A similar sharp decrease due to a small amount of additive was also observed by other authors. For example, Khalil et al.[13] reported that the addition of 1 wt% of TiO_2 caused a 9% decrease in dielectric-breakdown strength of LDPE. The breakdown strength, E_0, of dried nanoscale TiO_2/LDPE was 3.51 MV/cm, close to that of neat LDPE. It is worthwhile noticing that at higher breakdown strength, the curves were almost superimposed. For dried nanoscale TiO_2/LDPE, the long low breakdown strength tail is thought to be due to the presence of agglomerates. As discussed below, there were some agglomerates at the size of a few micrometers in the sample. If several such agglomerates happened to be just underneath the spherical electrode (contact area of the high potential spherical electrode with the sample was about 0.4 mm^2) and nearly aligned in the electric field direction, the field enhancement could be quite high considering that the sample thickness was in the range of 10–40 μm. In this case, the breakdown channel would form at a much lower external electric field, and the sample would therefore yield

TABLE I. Comparison of the breakdown strength (BD) and the data scatter for LDPE and various LDPE-based composites.

Sample	Average BD (MV/cm)	Standard error (MV/cm)	E_0 (MV/cm)	β	Data amount
Unifilled LDPE	3.37	1.14	3.78	3.53	22
LDPE/5 wt% as-received micrometer-TiO_2	2.02	0.59	2.24	3.98	23
LDPE/5 wt% as received nano-TiO_2	2.10	0.50	2.30	5.12	30
LDPE/5 wt% dried micrometer-TiO_2	2.41	0.64	2.58	4.51	34
LDPE/5 wt% dried nano-TiO_2	3.12	1.13	3.51	3.03	23
LDPE/5 wt% AEAPS–TiO_2	2.75	0.78	3.13	3.31	24

E_0, Weibull breakdown strength; β, a shape parameter of Weibull distribution; LDPE, low-density polyethylene; AEAPS, *N*-(2-aminoethyl) 3-aminopropyltrimethoxysilane.

unusually low breakdown strength values. The high breakdown strength values in the dried nanoscale TiO_2/LDPE correspond to regions with well-dispersed dried small nanoparticles. Due to a partial overlap of the 95% confidence bounds, the breakdown strength of the samples containing dried nanoscale TiO_2 was not significantly different from that of unfilled LDPE. However, the difference in breakdown strength between the as-received and dried nanoscale TiO_2/LDPE composites was significant, indicating that drying the nanoparticle surface had a significant effect on the breakdown strength.

The surface of oxide nanoparticles is always covered by hydroxyl groups (M–OH) and molecularly adsorbed water hydrogen-bonded to the surface. Thermogravimetry (TGA) was used to investigate the oxide surface before and after the drying treatment. It was found (Fig. 2) that drying at 195 °C efficiently removed most of the surface water as shown by the lack of weight loss below 300 °C after drying.[19] The weight loss continued until over 800 °C indicating that there were still hydroxyl groups on the surface.[20] If we assume the difference in weight loss at 300 °C was due to the removal of the molecularly adsorbed water layer (not including trapped molecular water) on the nanoparticle surface, then the surface water accounted for about 0.93 wt% in as-received nanoscale TiO_2. When 5 wt% as-received nanoparticles were put into the polymer matrix, the overall water content in the resulting composite samples went down to as low as 0.047 wt%. It is worthwhile to consider how such a small amount of water has such a significant effect on the breakdown strength. Some possible reasons are presented. First, drying the surface led to a better interface because the surface was less hydrophilic, as observed by the ease with which the dried particles floated on water, whereas the wet ones sink. Due to the same reason of the improved compatibility, dried nanoscale TiO_2 exhibited a better dispersion in the matrix, which showed a much finer fracture pattern as seen in Fig. 3. Very small nanoparticles could not be seen easily

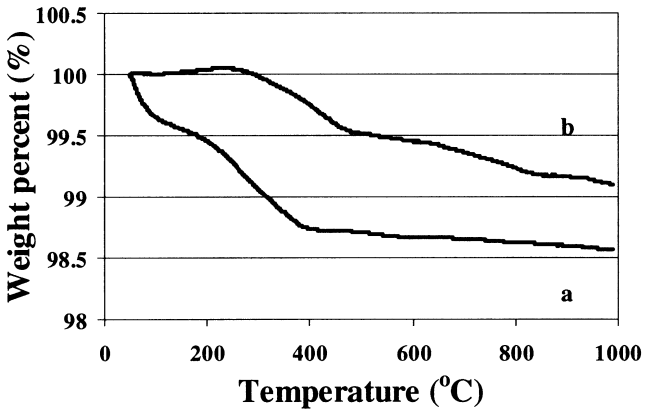

FIG. 2. Weight loss of pure TiO_2 nanoparticles (a) before and (b) after drying treatment as a function of temperature (after Ref. 19).

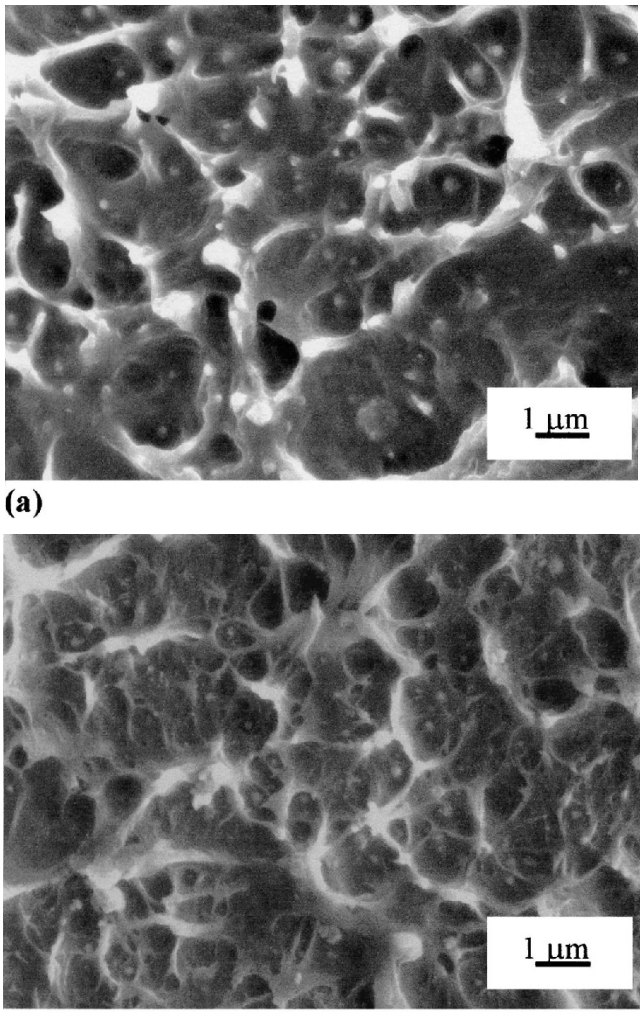

FIG. 3. FE-SEM images showing the dispersion of (a) as-received TiO_2 nanoparticles and (b) dried TiO_2 nanoparticles in LDPE.

at such small concentration by FE-SEM because they tend to be covered by the polymer. Therefore, we paid more attention to the number and size of larger agglomerates. Both samples had some, not many, agglomerates. As-received nanoscale TiO_2 formed more and larger agglomerates in the matrix, and its samples showed a coarser fracture pattern. The largest agglomerate found for as-received nanoscale TiO_2-filled samples was over 10 μm in diameter. The size of most agglomerates generally did not exceed a few micrometers in both samples. The surface of both samples, however, showed good dispersion (Fig. 4). The reason that we paid attention to the surface dispersion was that the field was strengthened near the sphere electrode edge; in this case, if the surface had a large defect (agglomerate) under the sphere electrode, the sample would exhibit electrical breakdown at a lower voltage.

In addition, morphology changes may contribute to the increase of the breakdown strength of dried nanoscale

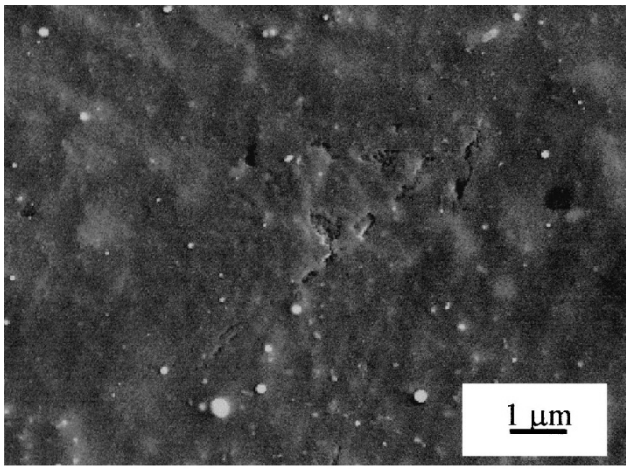

(a)

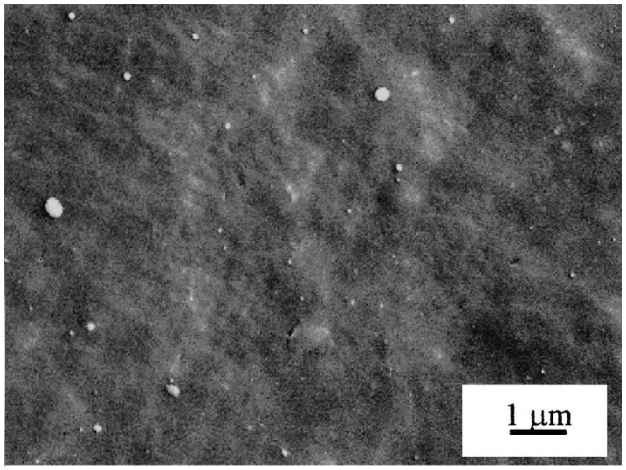

(b)

FIG. 4. FE-SEM images showing the surface dispersion of (a) as-received TiO_2 nanoparticles and (b) dried TiO_2 nanoparticles in LDPE.

TiO_2-filled samples compared with as-received nanoscale TiO_2-filled samples. It is quite possible that nanoscale TiO_2 acts as a nucleation site and promotes heterogeneous nucleation of LDPE.[21] Both lamellar thickness and its distribution could vary based on the surface chemistry of nucleation centers, which may influence the breakdown strength. Our results from DSC measurements (Table II), however, showed no change in weight average lamellae thickness. But one needs to be very careful when analyzing lamellae thickness using DSC because the analysis excludes many considerations such as melting, recrystallization, and thermal lag. In our case, it was even more complicated with the presence of nanoparticles, and we did not take into account parameter changes such as surface energy due to the presence of nanoparticles. Although DSC cannot yield absolute values of the lamellar thickness, it provides an easy way to compare relative lamellar thickness. Visual observation of the lamellae by AFM verified the above conclusion

TABLE II. Crystallinity, lamellae thickness, and melting behavior obtained by DSC and XRD analysis.

	DSC				XRD
Sample	α_c (%)	$T_{m,p}$ (°C)	W_P (°C)	l_w (nm)	α_c (%)
Unfilled PE	45 ± 1	112.3 ± 0.3	7.6 ± 0.2	5.86 ± 0.02	39
TiO_2/PE	47 ± 2	112.2 ± 0.2	7.6 ± 0.4	5.82 ± 0.03	32
Dried TiO_2/PE	45 ± 2	112.0 ± 0.3	8.1 ± 0.6	5.76 ± 0.06	39

α_c, crystallinity; $T_{m,p}$, peak melting temperature; W_p, width of the melting peak; l_w, weight average of lamellae thickness; DSC, differential scanning culorimetry; XRD, x-ray diffraction; PE, polyethylene.

that the average lamellar thickness was nearly the same for all three samples: unfilled LDPE and LDPE composites filled by the as-received or dried TiO_2 nanoparticles. In addition, supermolecular structures including the size, shape, and organization of spherulites may vary. Khalil[21] reported the modification of morphology due to the introduction of TiO_2 fine particles. Hosier et al.[18,22] demonstrated that microstructural features of polymers could have a marked influence on the macroscopic breakdown strength. In our case, preliminary AFM observations showed that both unfilled LDPE and dried TiO_2-filled LDPE samples exhibited a well-defined impinging spherulite structure [Fig. 5(a)]. However, in as-received TiO_2-filled samples, only immature spherulites or mostly lamellar sheaf-like structures were observed from the AFM images obtained to date [Fig. 5(b)]. The disruption of the regular supermolecular structure in the as-received nanoscale TiO_2/LDPE was quite possibly due to the poor interface between the as-received TiO_2 nanoparticles and the polymer. We believe that this disruption of regular supermolecular structures in the as-received TiO_2-filled samples is an important reason for the decrease in their electrical breakdown strength. The changes of morphologies, however, need not be expressed as a change in crystallinity. Our DSC and XRD studies (Table II) both revealed similar crystallinity for unfilled LDPE, as-received nanoscale TiO_2, and dried nanoscale TiO_2-filled LDPE. The DSC thermograms are shown in Fig. 6.

Finally, the conductive water layer itself on the nanoscale TiO_2 surface may cause conductive power loss. This could result in an increase of temperature locally, causing burning and decomposition of the surrounding polymer, thus leading to thermal breakdown. In addition, the conductive water layer may further increase the local field distortion and lead to breakdown across the interface. To verify the effect of the water layer itself on the electrical breakdown strength due to its electrical characteristics, including all the above-mentioned factors, we mixed octadecylamine, a surfactant, with the as-received and dried nanoparticles by sonicating them in xylene, then mixed the resultant suspension with a hot LDPE/xylene solution. The polar end of the surfactant was attracted by the nanoparticle surface, whereas the hydrophobic end

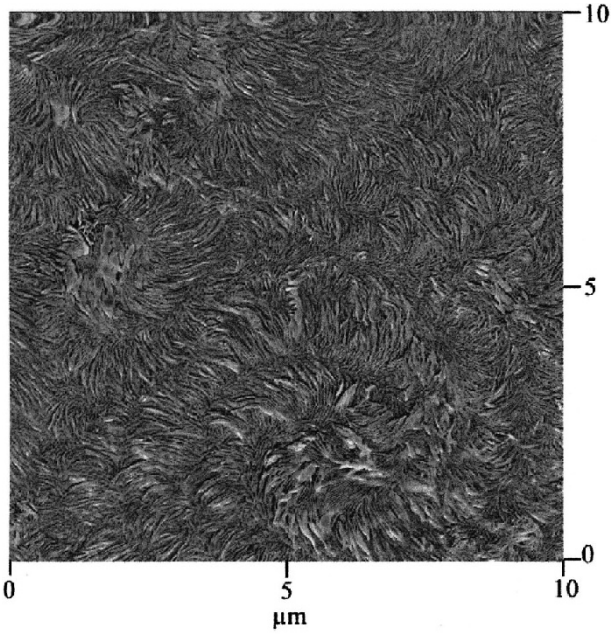

(a)

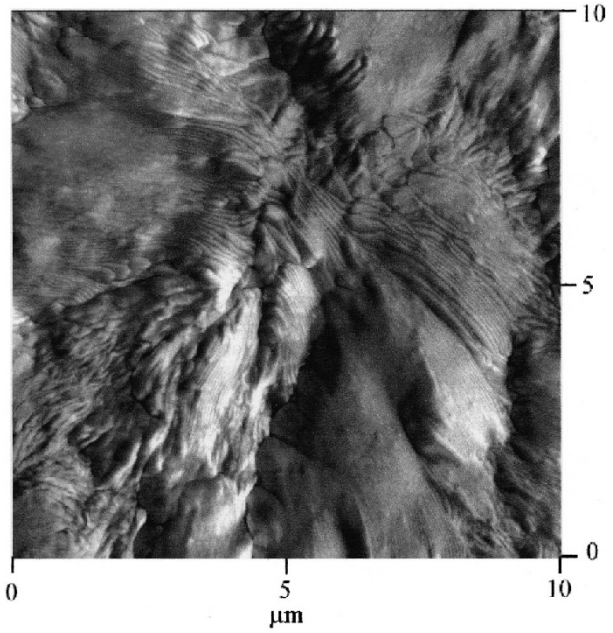

(b)

FIG. 5. AFM phase images in tapping mode of (a) neat LDPE and (b) LDPE filled with as-received TiO_2 nanoparticles.

created a compatible interface between the nanoparticles and the polymer matrix. By using the above strategy, we fabricated two systems having the same interface features with the main, if not only, difference being the presence of the water layer. Preliminary results showed that the difference in the electrical breakdown strength in these two systems was not significant. This indicated that

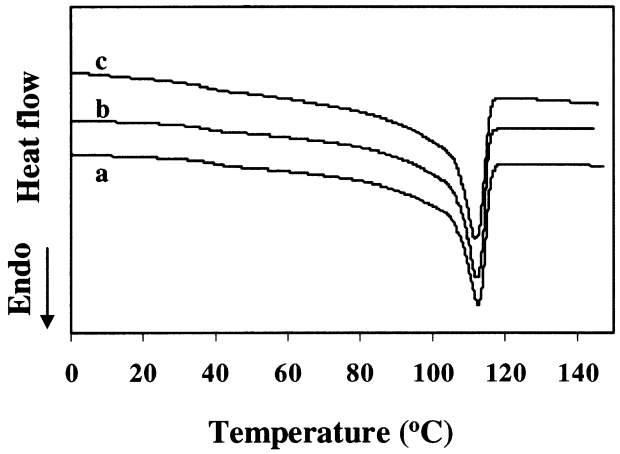

FIG. 6. DSC melting curves for (a) neat LDPE and LDPE filled with (b) as-received, and (c) dried TiO_2 nanoparticles.

the water layer itself did not play an important role in the breakdown behavior of samples. Therefore, the sharp increase in the electrical breakdown strength of the dried samples compared with the as-received samples did not result directly from the removal of the water layer, but was due to other changes related to the removal of the water layer such as the morphology and interface changes. More work needs to be done to understand fully the operative mechanism or mechanisms. In addition, please note that the difference between the silane coating and the surfactant is that the surfactant will not consume the surface water. So ideally, it maintained the initial surface status of both as-received and dried TiO_2 particles.

The effect of drying particles on breakdown strength was also examined for microscale TiO_2-filled LDPE samples. Dried microscale TiO_2/LDPE samples showed only a slightly higher breakdown strength than as-received microscale TiO_2/LDPE samples, and the difference was not significant. Our TGA results indicated that even for as-received microscale TiO_2, its surface was quite dry (water content was less than 0.1 wt%). Drying only further removed the small amount of water. In addition, the surface area of microscale TiO_2 was much smaller than that of nanoscale TiO_2. This means that the interfacial zone, which is a transition region between the particles and the bulk polymer matrix, accounts for less volume fraction in the microcomposite samples than in the nanocomposite samples. Therefore, the surface characteristics of microscale TiO_2 were not expected to act as an important factor in determining the final properties of these samples. Due to the above two reasons, the drying process did not play a significant role in this microcomposite system.

Table I also compares E_0 values for unfilled PE, as-received nanoscale TiO_2-filled LDPE, and AEAPS-coated nanoscale TiO_2-filled PE. AEAPS accounted for

about 2.8 wt% of the coated particles from our TGA experiment, and the surface coverage was estimated as 6.8 μmol/m^2. ^{29}Si nuclear magnetic resonance measurements verified that AEAPS mainly covalently bonded to the TiO_2 surface. The detailed results of the coating structure characterization have been submitted elsewhere for publication.[19] After such surface modification, E_0 was still lower than that for unfilled LDPE. However, it was about 40% higher than that for uncoated, as-received nanoscale TiO_2-filled PE, although the dispersion was much worse in the samples filled by the coated than by the uncoated particles. For the coated-particle composites, agglomerates could be seen with the naked eye. This indicated that other features related to particle surfaces had a more important influence on E_0 than dispersion here. In this case, the increase of E_0 was quite possibly due to an increase in electron scattering in the samples owing to the existence of polar groups in AEAPS. The result is promising. We can expect that by choosing a very "good" coupling agent (which can strengthen electron scattering, give a good interface, and yield a good dispersion), an E_0 can be obtained that can be even higher than that of neat LDPE.

To characterize fully the breakdown strength, not only E_0, but also the spread of the data has to be considered. According to Ref. 15, the shape parameter β [Eq. (1)] determined by the linear regression method represents the spread of breakdown strengths: β tends to decrease with an increase in scatter. Our results (Table I) show the same trend by comparing β values with the standard deviation. The β values ranged from 3 to 6. Similar values were reported by Dissado et al.[23] for polyethylene under ac conditions. Note the dried or AEAPS-coated nanoscale TiO_2-filled samples showed higher scatter than that of unfilled LDPE whereas the samples filled with as-received nanoscale TiO_2 or the dried micrometer-scale TiO_2 showed lower scatter than that of unfilled LDPE. A similar phenomenon, that composites showed lower scatter than the unfilled matrix, had been reported by Ueki and Zanin.[15]

IV. CONCLUSIONS

In summary, surface chemistry, such as the presence of surface water or surface silane, has a significant influence on the breakdown strength. The reason that the surface can play such an important role in nanocomposites is the large surface area possessed by the nanoparticles. By using dried nanoscale TiO_2, the breakdown strength (E_0) at the cumulative failure probability of 63.2% was increased by 50% compared with the samples filled by the as-received nanoscale TiO_2, close to that of unfilled LDPE. AEAPS-coated nanoscale TiO_2-filled samples showed a nearly 40% increase in E_0 compared with that of uncoated, as-received nanoscale TiO_2-filled samples.

ACKNOWLEDGMENTS

The work was supported by the ABB AB and the Nanoscale Science and Engineering Initiative of the National Science Foundation under NSF Award No. DMR-0117792. We would also like to acknowledge the Mettler-Toledo Thermal Analysis Education Grant 2001 for the use of thermogravimetric analysis. We would also like to thank Prof. Yvonne Akpalu for all her discussions about morphology.

REFERENCES

1. Y. Tanaka, N. Ohnuma, K. Katsunami, and Y. Ohki, IEEE Trans. Electr. Insul. **26,** 258 (1991).
2. R. Hackam, IEEE Transactions on Dielectrics and Electrical Insulation **6,** 557 (1999).
3. M. Ieda, IEEE Transactions on Dielectrics and Electrical Insulation **21,** 793 (1986).
4. D. Ryfšavý and H. Tkadlečková, Polym. Degrad. Stabil. **37,** 19 (1992).
5. R. Gächter and H. Müller, *Plastics Additives Handbook* (Hanser Publishers, Munich, 1990).
6. A.C. Ashcraft, R.M. Eichhorn, and R.G. Shaw, in *Conference Record of the 1976 IEEE International Symposium on Electrical Insulation* (IEEE, Montreal, Canada, 1976), p. 213.
7. Y. Yamano and H. Endoh, IEEE Transactions on Dielectrics and Electrical Insulation **5,** 270 (1998).
8. M.H. Sabuni and J.K. Nelson, J. Mater. Sci. **14,** 2791 (1979).
9. C.C. Ku and R. Liepins, *Electrical Properties of Polymers: Chemical Principle* (Hanser Publishers, Munich and New York, 1987).
10. M.S. Khalil, IEEE Transactions on Dielectrics and Electrical Insulation **7,** 261 (2000).
11. G. Chen and A.E. Davies, IEEE Transactions on Dielectrics and Electrical Insulation **7,** 401 (2000).
12. S. Fujita, M. Ruike, and M. Baba, in *Conference on Electrical Insulation and Dielectric Phenomena* (IEEE, San Francisco, 1996), p. 738.
13. M.S. Khalil, P.O. Henk, and M. Henriksen, in *Conference Record of the 1990 IEEE International Symposium on Electrical Insulation* (IEEE, Toronto, Canada, 1990), p. 268.
14. *Electrical Properties of Polymers*, edited by D.A. Seanor (Academic Press, New York, 1982).
15. M.M. Ueki and M. Zanin, IEEE Transactions on Dielectrics and Electrical Insulation **6,** 876 (1999).
16. B. Crist and F.M. Mirabella, J. Polym. Sci. B, Polym. Phys. **37,** 3131 (1999).
17. S.L. Aggabwal and G.P. Tilley, J. Polym. Sci. **XVIII,** 17 (1955).
18. I.L. Hosier, A.S. Vaughan, and S.G. Swingler, J. Mater. Sci. **32,** 4523 (1997).
19. D. Ma, D.F. Rogers, N. Wu, B.J. Ash, R.W. Siegel, T. Apple, B.C. Benicewicz, and L.S. Schadler (unpublished).
20. M. Primet, P. Pichat, and M. Mathieu, J. Phys. Chem. **75,** 1216 (1971).
21. M.S. Khalil, J. Polym. Mater. **41,** 71 (1998).
22. I.L. Hosier, A.S. Vaughan, and S.G. Swingler, J. Polym. Sci. B, Polym. Phys. **38,** 2309 (2000).
23. L.A. Dissado, I. Doble, S.W. Wolfe, P.A. Norman, A.E. Davies, G. Chen, Q. Zhong, W.B. Wargotz, and M.M. Sanders, IEEE Transactions on Dielectrics and Electrical Insulation **4,** 1 (1997).